SLAC-PUB-17126

FURTHER UNDERSTANDING THE LCLS INJECTOR EMITTANCE*

F. Zhou,+ K. Bane, Y. Ding, Z. Huang, and H. Loos, SLAC, Menlo Park, CA 94025, USA

Abstract

Coherent optical transition radiation (COTR) from the laser heater chicane is recently observed at the OTR screen used for the injector emittance measurements at the Linac Coherent Light Source (LCLS). The injector emittance measured at the OTR screen is under-estimated by 30% due to the COTR effect. Slice emittance upstream of the first LCLS magnetic bunch compressor (BC1) is measured, 0.45 μm for a central slice beam, using a traditional transverse s-band radio frequency deflector. Slice x- and y-emittances downstream of the BC1 are measured using a recently developed technique. It makes use of a collimator in the BC1 center to select a small portion of beam as a time-sliced beam. The measured projected emittance for the slice beam is considered as the slice emittance. With the technique, the measured central slice y-emittance is 0.45 μm after the BC1, similar to the injector emittance before the BC1, but the measured so-called central slice x-emittance has about 20% of increase after the BC1. Further measurements and analyses reveal that the parasitic effects, including collimator wakes, longitudinal space charge and dispersion due to the introduction of the beam collimation, do not impact the measured slice x- and y-emittance but coherent synchrotron radiation (CSR) deteriorates the projected x-emittance of the slice beam. The measured projected x-emittance of a slice beam under the CSR condition cannot be considered as a slice x-emittance. The technique is capable of reliable measurements of a slice emittance in non-bending plane instead of the bending plane, when a beam transports through magnetic bunch compressors.

EMITTANCE AT 135 MEV, PRIOR TO THE BC1

The Linac Coherent Light Source (LCLS), located at the SLAC National Accelerator Laboratory, has been successfully operated for users for more than five years [1]. Accurately characterizing emittance particularly the injector emittance is of importance for the x-ray Free Electron Laser (FEL) operations. Figure 1 shows the major components of the LCLS injector and its first magnetic bunch compressor (BC1) [2]. It begins with a copper cathode s-band RF gun and two s-band linac sections producing an electron beam with energy of 135 MeV. The 135-MeV beam then passes through a small laser heater (LH) chicane, followed by an s-band transverse RF deflector for time-resolved beam measurements. The 135-MeV beam is measured by the emittance station consisting of three optical transition radiation (OTR) screens or wire scanners. Then the beam is transported into the main linac and accelerated to 240 MeV through the L1S before entering the BC1. Located between these two structures is the x-band RF structure to linearize the longitudinal phase space before the bunch compression. There are three wire scanners downstream of the BC1 for emittance measurements. The quadrupole scan is used to measure emittance for a 135 MeV beam with one OTR screen or wire-scanner, and for a 220 MeV compressed beam after the BC1 with one wire scanner. The bunch charge is 150 pC for all emittance measurement discussed in the context.

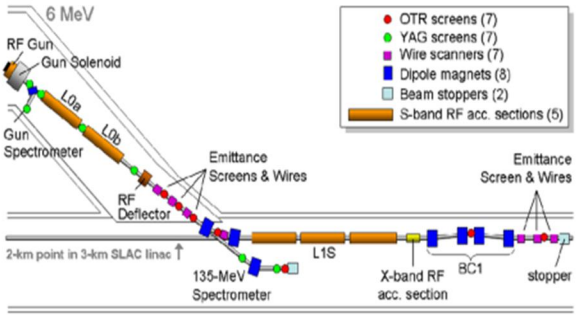

Figure1: Schematic layout of the LCLS injector including the BC1. The laser heater chicane is located in between the L0B and the RF deflector.

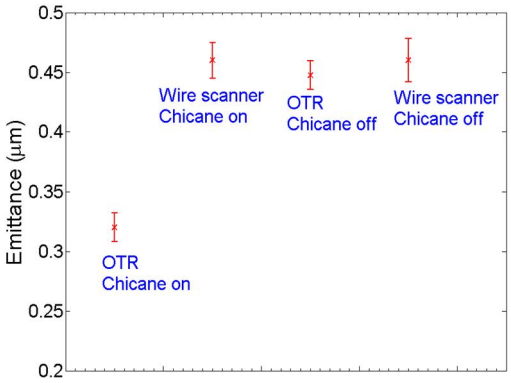

Figure 2: Projected emittance with the OTR screen and the wire-scanner for the LH chicane on and off at 135 MeV for 150 pC.

The LH chicane is to accommodate a short undulator for interaction of the laser beam with the electron beam to introduce an uncorrelated energy modulation of the electron beam to suppress the micro-bunching instability. The interaction of the electron beam with the laser beam in the LH chicane also induces micro-bunching at the laser wavelength and its harmonics, leading to coherent optical transition radiation (COTR) effects on the OTR screen [3] thereby impacting the accuracy of the emittance measurement. Therefore, the laser beam for the LH was always turned off but the LH chicane is normally

This material is based upon work supported by the U.S. Department of Energy, Office of Science, under Contract No. DE-AC02-76SF00515.

turned on during routine emittance measurements using the OTR screen. However, with the LH chicane-on, we recently observed that the integrated charge at the OTR screen is still changed by a factor of 2 during the quadrupole scan. The micro-bunching from the cathode and drive laser could be amplified through the small R_{56} (5 mm) of the LH chicane itself. It makes optical transition radiation coherently at the OTR screen downstream of the chicane. The coherent optical transition radiation (COTR) light makes the core of electron beam denser thereby resulting in smaller electron beam. Turning off the LH chicane the integrated charge at the OTR screen is similar for different quadrupole strength. Using the wire scanner, the integrated charge for different quadrupole strength is similar, for both the LH chicane-on and –off. It indicates the wire scanner is not subject to the COTR light. Figure 2 shows the emittance comparisons for the LH chicane-on and -off using the OTR screen and the wire scanner for 150 pC. It shows that the emittance using the wire scanner is similar to the one using the OTR with the LH chicane-off. The OTR emittance with the LH chicane-on is underestimated by about 30%. The slice emittance is measured using the transverse RF deflector with the OTR screen at 135 MeV, prior to the BC1, as shown in Fig. 3. It shows the central slice beam emittance is about 0.45 μm for 150 pC with the LH chicane-off, and the measured slice emittance is underestimated by 30% with the LH chicane-on. Presently, the wire scanner replaces the OTR screen for emittance measurements at the 135-MeV LCLS injector.

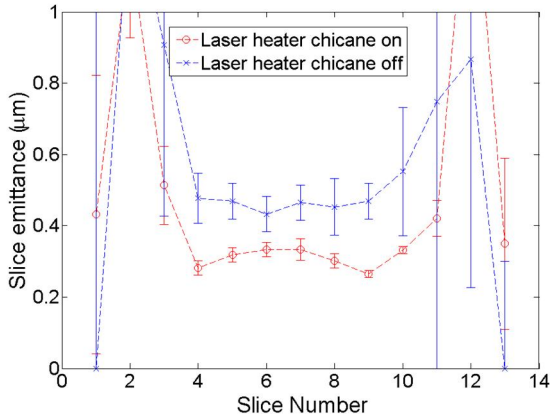

Figure 3: Slice emittance measured at the LCLS injector with the LH chicane-on and -off at 135 MeV, using the transverse RF deflector.

SLICE EMITTANCE MEASUREMENTS AND ANALYSES FOR THE BC1

It is crucial to measure and preserve the time-sliced beam emittance along the accelerator beamline particularly through the magnetic bunch compressors (BCs) for x-ray FEL operations. The transverse phase space volume of a slice beam may blow up, when an electron beam experiences non-linear fields along the beamline. Due to the lack of valid diagnostics for the time-sliced emittance measurements after the BCs at the LCLS, we used to assume that the slice emittance is kept unchanged from the injector to the undulator for prediction of the LCLS FEL performance. Recently, a simple collimation technique is developed to measure the time-sliced emittance at the FERMI [4] and the LCLS, which provides a possible solution to measure the slice emittances through the BCs.

The schematic layouts of the LCLS BC1 and the 2nd magnetic bunch compressor (BC2) are very similar, as shown in Fig. 4. The BC1 is used for the following descriptions. The electron beam is bent in the x-plane. The electron beam is chirped with an off-crest RF phase of L1S linac before entering the BC1 chicane. In the BC1, the beam is time-horizontal position correlated, when the energy-time correlated chirped beam passes through the horizontally dispersive region. The nominal chirped beam width at the middle of the LCLS BC1 is about 11 mm for nominal operation with 150 pC of bunch charge. A horizontally-flat collimator is situated in the middle of the BC1 chicane to scrape the electrons by changing the horizontal collimator gap. Figure 5 (top) shows the full chirped-beam image taken at the OTR screen immediately after the BC1 collimator. The dispersive beam size at the center of the BC1 is 2.3 mm, much larger than the betatron beam size of 90 μm. Thus, different width of time-sliced beams can be selected using the horizontal collimator jaws shown in Fig. 5 (middle and bottom). The projected emittance of selected time-sliced beam passing through the collimator is measured at 220 MeV, with a wire-scanner downstream of the BC1 using a quadrupole scan. The measured projected emittance of a small portion of the full beam is considered as the slice emittance with this technique.

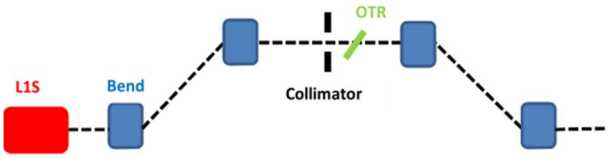

Figure 4: Schematic layout of the LCLS BC1. The collimator is situated in the center of the BC1 chicane and the OTR screen is next to the collimator. L1S is the linac used to introduce the energy-time correlation for the bunch compression.

Figure 6 shows the measured slice emittances in x- and y-plane through the BC1 with the collimation technique. The bunch charge before the collimation is 150 pC. The central slice beam charge is about 10 pC with 0.5 mm of the collimator gap. The measured central slice y-emittance through the BC1 is about 0.45 μm similar to the one before the BC1, while the measured so-called slice x-emittance is increased by about 20%. Similar phenomena are observed at the LCLS BC2, although the relatively large energy jitter makes the slice measurements jittery with the sub-mm collimator gap. This paper focuses on the measurements and analyses for the LCLS BC1. The following sections are to evaluate the parasitic effects of

using the collimation technique and discuss the so-called slice x-emittance growth.

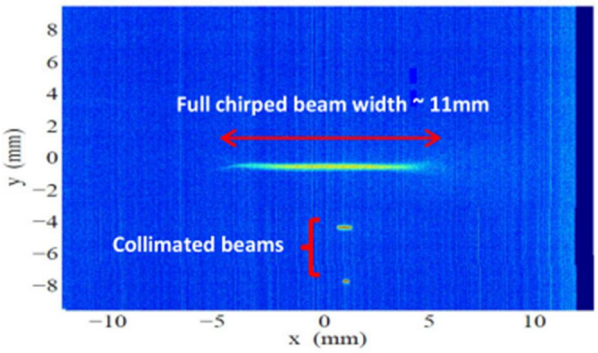

Figure 5: Example of the measured full chirped beam image at the OTR near the BC1 center (top) and sliced beams with different length after beam collimation (middle and bottom) at the LCLS BC1 with 150 pC.

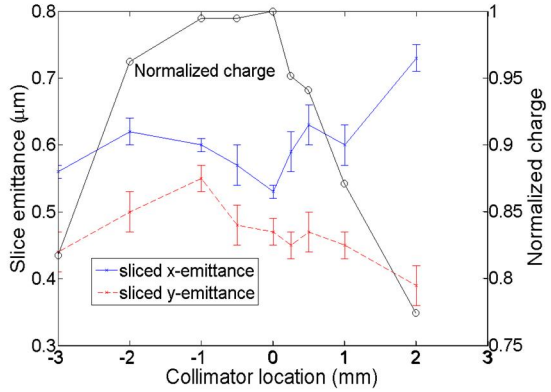

Figure 6: Time-sliced x- and y-emittances measured downstream of the LCLS BC1 at 220 MeV.

Impact of the X-Band Linearizer

The x-band linearizer, located upstream of the LCLS BC1, is used to linearize the longitudinal phase space of the chirped beam. A local x-bump is usually generated around the x-band cavity to reduce the wake effects, caused by the misalignments in the x-band structure. Figure 7 shows the measured projected and slice x-emittance as a function of transverse offset in the x-band cavity. In the full open state (10 cm of collimator gap), the measured emittance is for the full beam - projected emittance. For the mm or sub-mm of the collimator gap, a small portion of the beam is transported through the collimator. Thus the measured projected emittance is for a slice beam - slice emittance. The measurements show that the slice emittance is very similar for 0 mm, 0.5 mm and 1 mm of the transverse offsets in the x-band cavity, although the projected emittances of the full beams are very different with these transverse offsets. It is understood that the transverse wake of the x-band cavity generates a time-dependent head-tail force, which only impacts the projected emittance of the full beam, rather than its slice emittance.

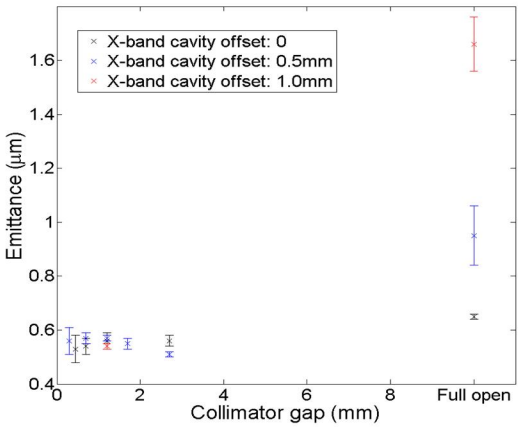

Figure 7: Measured projected and time-sliced x-emittance vs. transverse offset of the x-band linearizer.

Collimator Wakes

As discussed in the previous section, the typical full chirped beam width at the LCLS BC1 chicane center is about 11 mm with 150 pC for nominal operations. To evaluate the collimator geometrical wake effects, the collimator gap is set to different values, from a few mm to sub-mm, for emittance measurements. Figure 8 shows the measured emittance with variable collimator gaps. The slice x- or y-emittance is similar with different gaps below 6 mm. During the emittance measurements, the beam optics matching parameters are not changed at all for different gaps. It indicates no additional focusing is introduced by the collimator wake. For the case of very short bunches $\sigma_z << b$ (b is the half gap of the collimator), valid for our case, the flat collimator wake can be predicted with the optical model [5-6]. With the beam centered between the collimator jaws, the collimator wake induced beam defocusing is estimated with:

$$\frac{1}{f} = \frac{Z_0 c \pi}{24} \frac{eN}{b^2 (E/e)} \qquad (1)$$

where f is the effective optical focal length caused by the collimator wake (defocusing is in the plane of the collimation), $Z_0 \approx 377\ \Omega$, c is the speed of light, eN is the transmitted bunch charge through the collimator, and E is the electron beam energy. The focusing depends on position within the bunch, with the bunch head experiencing no effect and the tail experiencing the wake effect described by Eq. 1. With the LCLS BC1 parameters, beam energy E=220 MeV, the typical transmitted charge eN= 10 pC through the minimum gap of 0.5 mm (half gap b= 0.25 mm), the focal length created by the collimator wake is about 90 m, much larger than the few meters of the focal length of the magnetic lattice optics. It confirms that the measured beam matching parameters are not changed for different collimator gaps. The emittance growth in the x- and y-plane due to the collimator's quadrupole wake is approximately expressed by:

$$\frac{\varepsilon_{nx,ny}}{\varepsilon_{nx0,ny0}} = \sqrt{1+\left(\frac{\beta_{x,y}}{f}\right)^2} \qquad (2)$$

where $\varepsilon_{nx0,ny0}$ and $\varepsilon_{nx,ny}$ are the original and final emittances respectively, and $\beta_{x,y}$ is the betatron function at the collimator. With nominal $\beta_{x,y}$=7 m, the emittance growth caused by the collimator quadrupole wake is <1%. Further calculations find that the resistive wall wake effect of the collimator is even weaker than the collimator's geometrical wake. The measurement and analysis lead to the conclusion that the contribution of the collimator wakes to the projected x- and y-emittance of a slice beam is negligible.

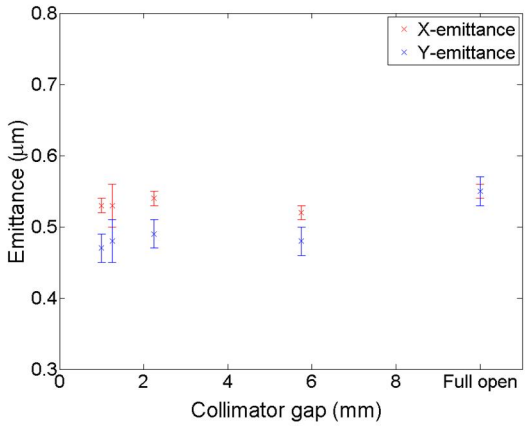

Figure 8: Measured x- and y-emittance vs. collimator gap. Full open means 100 mm of the collimator gap.

Dispersion Effect

In practice, <1 cm of the x-dispersion leakage from the LCLS BC1 chicane is possible. The dispersion induced x-emittance growth is estimated by:

$$\frac{\Delta\varepsilon_x}{\varepsilon_{x0}} \approx \frac{1}{2}\frac{(\eta_x \cdot \delta_E)^2}{\beta_x \cdot \varepsilon_{x0}} \qquad (3)$$

where $\Delta\varepsilon_x$ is the emittance growth, ε_{x0} is the initial un-normalized emittance, β_x is the betatron function at the emittance measurement station, η_x is dispersion and δ_E is the rms energy spread. For the BC1 collimation measurements, only <5% of the full beam is selected for one slice beam measurement. Thus, the rms energy spread of a slice beam is about 0.05% for 1% of the rms energy spread for a full beam. Substituting the parameters into the Eq. 3 gives 1% of x-emittance growth for a slice beam with the 0.45 μm of the initial normalized slice x-emittance.

Longitudinal Space Charge and Coherent Synchrotron Radiation Effects

The longitudinal space charge (LSC) can degrade longitudinal phase space and transverse phase spaces in both x- and y-plane simultaneously. In the collimation scheme, the electron beam is truncated in the dispersion region or energy dimension, which makes the collimated beam current profile to a flat-top shape but with certain slope on both edges. For this change, the LSC effect [7] is evaluated. Using the simulated temporal profile, we calculated the LSC and the emittance growth with the beam collimation and found the effects are negligible. The measured well-preserved slice y-emittance from the 135-MeV injector to the BC1, as stated in the previous sections, verifies the LSC is not the cause of the slice x- and y-emittance growth.

Short electron bunches traversing a dipole with bending radius ρ can emit coherent synchrotron radiation (CSR) [8-9] at wavelengths longer than the bunch length. Figure 9 shows the measured projected x- and y-emittance and slice y-emittance as function of the L1S phase for different bunch compressions. The CSR causes significant projected x-emittance growth at -30°, with which the beam is near full compression. It also shows that the measured central slice y-emittance using the collimator technique is similar for different bunch compressions, close to 0.45 μm measured at 135 MeV before the BC1. 0.5 mm of the collimator gap is used for all slice beam measurements. The selected slice beam length basically matches with FEL process in the undulator. The measured projected x-emittance of a collimated slice beam is grown by about 20% for the under-compression (-27°). Similar projected x-emittance growth for a slice beam was observed in Ref. [4] with the same collimation technique. The CSR caused x-emittance growth for a collimated slice beam can be estimated with 1D steady-state model:

$$\varepsilon_{xn} = \varepsilon_{xn0}\sqrt{1+\left(\frac{\theta}{2}\frac{\delta_{CSR}}{\sigma_{x0}'}\right)^2} \qquad (4)$$

where ε_{xn} and ε_{xn0} are the final and initial emittances respectively, θ is the bending angle, 0.1 rad, σ_{x0}' is the original beam divergence, and δ_{CSR} is the CSR caused rms energy spread expressed by:

$$\delta_{CSR} \approx 0.532\frac{Q}{E}\frac{Z_0 cL}{2\times 3^{4/3}\pi\rho^{2/3}\sigma_z^{4/3}} \qquad (5)$$

where L is the bend length, 0.2 m, and ρ is the bending radius, 2 m, E is the beam energy at the BC1, 220 MeV, Q and σ_z are the bunch charge and bunch length respectively after the collimation, Z_0 =377 Ω, and c is the speed of the light. With 0.5 mm of the collimation, the bunch charge Q and bunch length σ_z are about 11 pC and 5 μm rms for under-compression (-27°). The calculations of the CSR for the last bend, applying above parameters into Eqs. 4-5, show that the projected x-emittance of the slice beam is grown by about 8%. The simulations using Elegant code predicts similar emittance growth with introducing 0.5 mm of beam collimation. Theoretical estimate and simulations verify the observed projected x-emittance growth for a collimated slice beam due to the CSR effect. Further simulations show that, without introducing the beam collimation, the time-sliced x-emittance is not changed for different bunch compressions. In the case of without beam collimation,

the CSR only impacts the head-tail of the electron beam (projected emittance of the full beam), and thus the slice emittance is not impacted. We conclude that under the CSR condition the measured projected x-emittance of a slice beam with the collimation technique cannot be considered as a slice x-emittance.

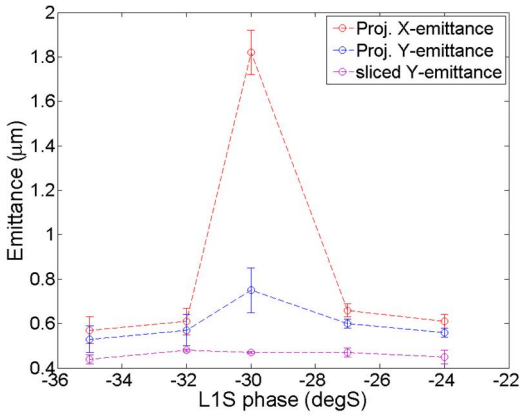

Figure 9: Projected x- and y-emittance and slice y-emittance for different bunch compressions with 150 pC.

SUMMARY

The LCLS injector emittance is under-estimated by 30% using the OTR screen due to the COTR effects from the LH chicane. With the transverse s-band RF deflector, the central slice emittance at 135 MeV prior to the BC1 is measured, about 0.45 μm for 150 pC. Emittances in the x- and y-plane for a slice beam through the BC1 are measured using a collimator located in the BC1 chicane center. With the collimation technique, the measured projected emittance for a slice beam is considered as the slice emittance. The measured so–called central slice x-emittance is increased by about 20% through the BC1, while the measured central slice y-emittance is about 0.45 μm similar to the one before the BC1. The further measurements and analyses reveal that the parasitic effects, including collimator wakes, longitudinal space charge and dispersion due to the introduction of the beam collimation, do not impact the measured projected x- and y-emittance of a slice beam but CSR effect deteriorates the projected x-emittance of the slice beam. Under the CSR condition, the measured projected x-emittance of a slice beam cannot be considered as a slice x-emittance. The technique is capable of reliable measurements of a slice emittance in non-bending plane instead of the bending plane, when a beam transports through magnetic bunch compressors.

*The work is supported by U.S. DOE under grant No. DE-AC02-76SF00515.

REFERENCES

[1] P. Emma *et al.*, "First Lasing and Operation of an Angstrom-wavelength Free Electron Laser", Nature Photon. 4, 641 (2010).

[2] R. Akre *et al.*, "Commissioning the Linac Coherent Light Source Injector", Phys. Rev. ST Accel. Beams 11, 030703 (2008).

[3] H. Loos *et al.*, "Observation of Coherent Optical Transistion Radiation in the LCLS Linac", in Proc. of 30th International Free Electron Laser conference, Gyeongju, Korea, 2008, pp. 485-489.

[4] S. Di Mitri, D. Castronovo, I. Cudin, and L. Frohlich, "Electron Slicing for the Generation of Tunable Femtosecond Soft X-ray Pulses from a Free Electron Laser and Slice Diagnostics", Phys. Rev. ST Accel. Beams 16, 042801 (2013).

[5] G. Stupakov, K.L.F.Bane, and I. Zagorodnov, "Optical Approximation in the Theory of Geometric Impedance", Phys. Rev. ST Accel. Beams 10, 054401 (2007).

[6] K.L.F.Bane, G. Stupakov, and I. Zagorodnov, "Impedance Calculations of Nonaxissymmetric Transitions using the Optical Approximation", Phys. Rev. ST Accel. Beams 10, 074401 (2007).

[7] A. Chao and M. Tigner (eds.), "Handbook of Accelerator Physics and Engineering", world scientific, Singpore, 1999. ISBN: 978-981-4415-84-2.

[8] J. Murphy, S. Krinsky, and R. Gluckstern, "Longitudinal Wakefield for an Electron Moving on a Circular Orbit", Particle accelerator 57 (1997), pp. 9-64.

[9] H. Braun *et al.*, "Emittance Growth and Energy Loss due to Coherent Synchrotron Radiation in a Bunch Compressor", Phys. Rev. ST Accel. Beams 3, 124402 (2000).